

## Resonant coupling of quantum dot intersublevel transitions with midinfrared photonic crystal modes

E. Homeyer,<sup>1</sup> J. Houel,<sup>1</sup> X. Checoury,<sup>1</sup> F. Delgehier,<sup>1</sup> S. Sauvage,<sup>1,a)</sup> P. Boucaud,<sup>1,b)</sup> R. Braive,<sup>2</sup> L. Le Gratiet,<sup>2</sup> L. Leroy,<sup>2</sup> A. Miard,<sup>2</sup> A. Lemaître,<sup>2</sup> and I. Sagnes<sup>2</sup>

<sup>1</sup>*Institut d'Electronique Fondamentale, CNRS-Univ Paris-Sud 11, Bâtiment 220, 91405 Orsay, France*

<sup>2</sup>*Laboratoire de Photonique et de Nanostructures, Route de Nozay, 91460 Marcoussis, France*

(Received 10 June 2009; accepted 8 July 2009; published online 28 July 2009)

We show that quantum dot intersublevel transitions can be coupled to midinfrared photonic crystal modes. The coupling is observed under optical pumping with *S-P* intersublevel transitions of InGaAs self-assembled quantum dots resonant around 20  $\mu\text{m}$  wavelength. An enhancement in the intersublevel absorption and a spectral tuning are evidenced when the optical modes of two-dimensional photonic crystals enter in resonance with the photoinduced intersublevel absorption. This effect is illustrated in the case of GaAs two-dimensional photonic crystal membranes with lattice periodicities of 10.5, 9.5, and 8.5  $\mu\text{m}$  containing multilayers of self-assembled quantum dots. © 2009 American Institute of Physics. [DOI: 10.1063/1.3189812]

Intersublevel transitions of semiconductor self-assembled quantum dots are optical transitions which can be used for midinfrared optical devices such as quantum dot infrared photodetectors,<sup>1–5</sup> focal plane arrays<sup>6,7</sup> or midinfrared emitters.<sup>8</sup> One of the most studied intersublevel transition is the transition between the *S* ground state to the first *P* excited state. This *S-P* transition is polarized in the layer plane of the quantum dots and exhibits a large dipole matrix element. In the case of InGaAs/GaAs self-assembled quantum dots, this transition is resonant around 20  $\mu\text{m}$  wavelength.<sup>9,10</sup>

Two-dimensional photonic crystals are known to modify the optical density of states.<sup>11,12</sup> They lead to a strong modification of light-matter interaction and can significantly enhance the absorption/gain and optical nonlinearities.<sup>13</sup> Photonic crystals can control the internal quantum efficiency of emitters through Purcell effects and can modify the far-field radiation pattern and extraction efficiency of the emission of embedded sources. A strong effort has recently been devoted to the analysis of quantum dot emitters in the near-infrared with photonic crystal or cavity modes. In the midinfrared spectral range, two-dimensional photonic crystals can be used to provide resonant cavities for lasers or to enhance absorption or spontaneous emission processes. At long wavelength, photonic crystals have been implemented to control the emission of terahertz quantum cascade lasers.<sup>14–16</sup> In the midinfrared, quantum dots are also candidates for laser emission since population inversion can be achieved through the engineering of the phonon-mediated relaxation rates.<sup>17</sup> The control of the interaction between photonic crystal modes and quantum dot intersublevel transitions represents a major step for the future development and optimization of midinfrared photonic devices with quantum dots.

In this work, we report on the coupling of *S-P* intersublevel transitions of InGaAs quantum dots with optical modes of two-dimensional photonic crystal membranes. As the optical transitions are resonant around 20  $\mu\text{m}$  wavelength, a

specific technological process has been developed in order to fabricate suspended photonic crystal membranes in a planar geometry. The fabrication process has been described in Ref. 18. The technological process requires a metallic film for wafer bonding. The photonic crystals thus cannot be studied at normal incidence in transmission geometry. We have thus studied the coupling of intersublevel transitions and photonic crystals through the emission port of a spectrometer.

Two distinct samples have been investigated. The reference sample (7am55) contains 80 InGaAs quantum dot layers separated by 50 nm thick GaAs barriers. The quantum dots are nominally undoped. The photonic crystal sample (77m05) consists in a 3  $\mu\text{m}$  thick GaAs membrane containing 30 quantum dot layers. The quantum dot layers are nominally doped with one carrier per dot. Air holes are etched through the membrane following a two-dimensional triangular lattice pattern. The lattice periodicities *a* are 10.5, 9.5, and 8.5  $\mu\text{m}$ . The air hole radius is  $r/a=0.35$ . The photonic crystal pattern extends over a surface of approximately  $100 \times 100 \mu\text{m}^2$ . The 3  $\mu\text{m}$  thick GaAs membrane corresponds to a  $\lambda/2n$  layer for 20  $\mu\text{m}$  wavelength. The membrane is separated from the GaAs substrate by a 7  $\mu\text{m}$  air gap. The GaAs substrate interface is covered by a AuIn<sub>2</sub> metallic layer for wafer bonding.

Reflectivity measurements were performed at room temperature using a microscope coupled to the Fourier transform spectrometer.<sup>18</sup> The coupling between intersublevel absorption and photonic crystal modes was studied at low temperature. For these experiments, the quantum dots were populated using a mechanically chopped continuous wave interband optical pumping at 850 nm in resonance with the wetting layer states. The incident intensity was around  $500 \text{ W cm}^{-2}$  corresponding to a photoinduced carrier density of less than one carrier per dot if we account for a 1 ns recombination time. Only transitions from the *S* ground state are expected to contribute in the low temperature experiments. The emission or photoinduced absorption was probed by collecting light at normal incidence with gold-coated mirrors with a 0.2 numerical aperture from the emission port of the spectrometer operated in step scan mode. An important feature is the sign and phase of the signal which is measured

<sup>a)</sup>Electronic mail: sebastien.sauvage@ief.u-psud.fr.

<sup>b)</sup>Electronic mail: philippe.boucaud@ief.u-psud.fr. URL: <http://pages.ief.u-psud.fr/QDgroup>.

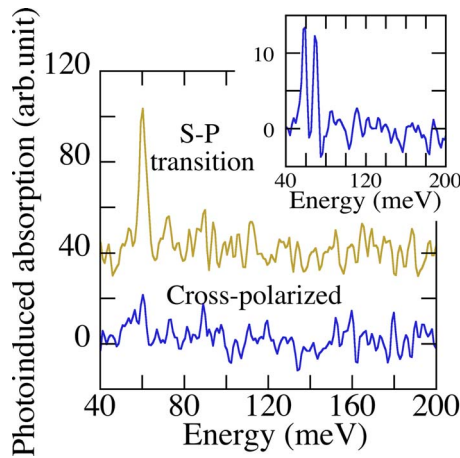


FIG. 1. (Color online) 77 K photoinduced absorption of a reference quantum dot sample (7am55) for two distinct linear orthogonal polarizations. The resonance at 60 meV is associated with the *S-P* intersublevel absorption. The curves have been offset for clarity. The inset shows a similar measurement performed at lower temperature (20 K). An additional resonance is observed at higher energy. It is attributed to the intersublevel absorption in presence of holes.

by a lock-in amplifier. The midinfrared signal has an opposite sign compared to the photoluminescence signal. It indicates that the measured signal corresponds to an absorption signal even if the sample is placed on the emission port of the spectrometer. It corresponds to the modulation of the room temperature surrounding blackbody radiation incident on the sample which is measured by the large band mercury cadmium telluride detector through the spectrometer optics. This modulation results from the photoinduced carrier absorption.

Figure 1 shows the spectral dependence of the midinfrared signal measured at 77 K for the 80 dot layer reference sample (7am55). Only a narrow line at 60 meV with a 4 meV linewidth is observed. It corresponds to an absorption signal. This resonance is polarized along one direction as it can be evidenced through the measurement performed with a polarizer rotated by 90°. The resonance is attributed to one *S-P* quantum dot intersublevel absorption since the resonance energy around 60 meV for InGaAs quantum dots and the polarization properties are signatures of this origin.<sup>9</sup> It is interesting to observe that only the quantum dots are significantly populated with the interband optical pumping. No significant free carrier absorption is observed in the measurement, the small resonance in cross-polarization is associated with a nonperfect alignment of the polarizer along the crystal axis. The cross-polarized *S-P* intersublevel transition at lower energy is not observed because of the detector cutoff. The photoinduced absorption signal is dependent on the presence of electron and holes in the dots and consequently on the carrier capture and thermoionic emission. This can be observed by performing the same measurement at a lower temperature (20 K) which is shown in the inset of Fig. 1. In the latter case, two resonances also polarized along one direction are clearly observed. The additional resonance at 68 meV is attributed to the *S-P* absorption in presence of holes captured simultaneously with electrons in the same dot. The blueshift in the absorption in presence of holes is associated with the formation of excitons and results from the Coulomb interaction between carriers in the quantum dots. This effect has been discussed and described in Ref. 19. The spectral range

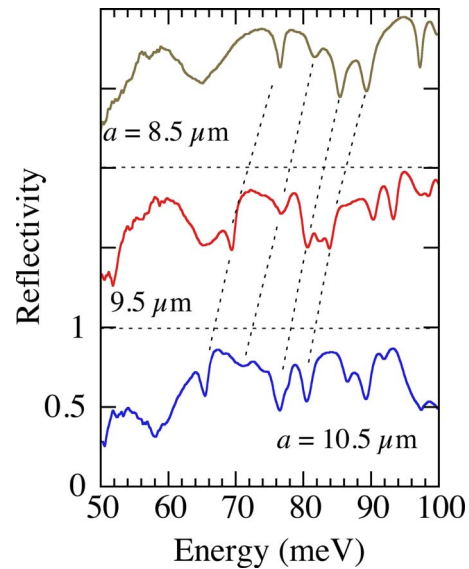


FIG. 2. (Color online) Room temperature reflectivity spectra of two-dimensional photonic crystal membranes (77m05). The bottom curve corresponds to a lattice periodicity of 10.5  $\mu\text{m}$ , the middle curve to 9.5  $\mu\text{m}$ , and the upper curve to a periodicity of 8.5  $\mu\text{m}$ . The curves have been offset for clarity. Some of the reflectivity resonances of the photonic crystals are highlighted including the low group-velocity band edge mode at 65 meV for the 10.5  $\mu\text{m}$  sample. The detector has a cutoff below 50 meV.

covered by the photoinduced intersublevel absorption is thus dependent on the carrier population of the quantum dots.

In order to couple photonic crystal and intersublevel transitions, one has to design photonic crystals with resonant optical modes around 20  $\mu\text{m}$ . The fabricated membrane-like photonic crystals exhibit such modes, as it can be observed by reflection microscopy. Figure 2 shows the room temperature reflection spectra of the photonic crystal membranes with three different lattice periodicities. These spectra are similar to those reported in Ref. 18 except that the resonances occur at longer wavelengths. The reflection spectra are a combination of broad Fabry–Perot resonances resulting from the vertical stacking of the membrane, air gap, and metallic bonding layers, and narrower resonances associated with the photonic crystal lattice. For the 10.5  $\mu\text{m}$  lattice periodicity, the reflectivity associated with a zone center low-group velocity mode is observed at 65 meV. The corresponding normalized frequency  $u = a/\lambda$  is 0.55. A two-dimensional plane-wave calculation of the band structure using an effective refractive index of 3 for a 3  $\mu\text{m}$  thick GaAs membrane in transverse electric polarization predicts the occurrence of zone center modes at 0.55. This mode shifts to 77 meV as the lattice periodicity is decreased to 8.5  $\mu\text{m}$  as seen in Fig. 2. Additional resonances are observed at higher energy in the three cases, reflecting the complexity of the band structure at high energy.

Figure 3 shows a comparison between the photoinduced absorption spectra of the photonic crystal region and the unpatterned region of sample 77m05. When the unpatterned region of the sample is illuminated, the signal is rather weak due to the smaller number of quantum dot layers as compared to the reference sample. One can however observe two resonances similar to those shown in the inset of Fig. 1 at 60 and 68 meV for the undoped sample. These resonances are peaked at 58 and 72 meV. The spectral shift as compared to the undoped 7am55 sample is attributed to the difference in the growth conditions and to the *n*-doping of the sample. In

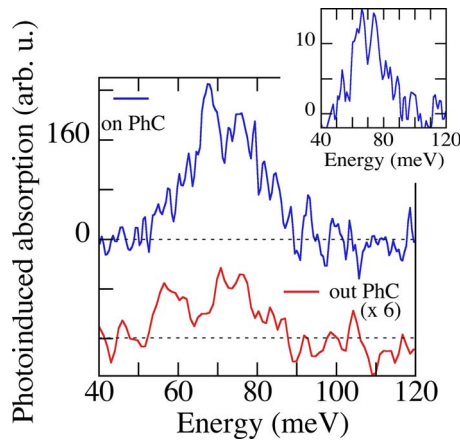


FIG. 3. (Color online) 77 K photoinduced absorption measured on the unpatterned area (lower curve) and on the photonic crystal (PhC) membrane with a 10.5  $\mu\text{m}$  lattice periodicity (upper curve). The curves have been offset for clarity. The origins are shown by dashed lines. The inset shows a measurement on the photonic crystal membrane measured with a lower resolution (2 meV).

Ref. 19, the calculated energy shift of the  $X^-$  excitonic transition (one hole and two electrons) as compared to the bare electronic transition was 4 meV larger than the energy shift in the  $X$  exciton. When the 10.5  $\mu\text{m}$  photonic crystal is illuminated, one observes a strong increase of the signal amplitude. This increase is also observed in the photoluminescence indicating that the trapping of the carriers and collection of the quantum dot emission are more efficient in the patterned area despite the nonradiative recombinations, which can occur at the photonic crystal side walls. The striking feature is the spectral modification of the photoinduced absorption. The spectrum is dominated by two resonances peaked at 67 and 75 meV. The amplitude ratio slightly depends on the excitation conditions as can be observed in the spectra at a lower resolution (2 meV) of the 10.5  $\mu\text{m}$  lattice parameter sample (inset of Fig. 3). There is thus a strong modification of the quantum dot intersublevel absorption through the photonic crystal patterning. The enhancement of the absorption around 67 meV is attributed to the slow-group velocity band-edge modes observed by room temperature reflectivity at 65 meV. The second resonance is associated with the modes observed at higher energy (72–75 meV) in the reflectivity spectra. The increased broadening as compared to the reflectivity spectra is associated to the lower resolution of the measurement on the emission port of the spectrometer and to the inhomogeneities of the photonic crystal lattice and optical pumping. The assignment of photonic crystal modes is supported by the comparison of the measurements between the samples with 10.5, 9.5, and 8.5  $\mu\text{m}$  lattice periodicities shown in Fig. 4. The photoinduced signal is similar for the samples with 10.5 and 9.5  $\mu\text{m}$  lattice periodicities, except for a blueshift of 3–4 meV when the lattice periodicity decreases. This blueshift is analog to the one observed in the reflectivity measurements. The signal is significantly decreased for the 8.5  $\mu\text{m}$  sample while the photoluminescence amplitude which gives an estimate of the quantum dot average carrier population is similar to the one of the other samples. Moreover, no peaked resonance is observed at 67–70 meV in the latter case. This is a consequence of the shift to high energy of the band edge mode which occurs for

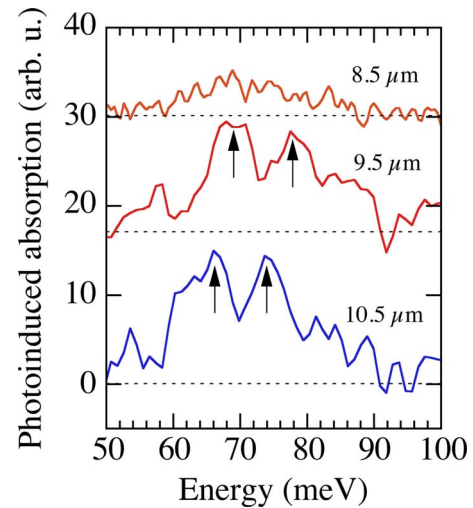


FIG. 4. (Color online) Comparison between the photoinduced absorption spectra of the photonic crystal membranes with 10.5, 9.5, and 8.5  $\mu\text{m}$  lattice periodicities. The temperature is 77 K. The blueshift in the resonances of the 10.5 and 9.5  $\mu\text{m}$  samples are highlighted by arrows. The curves have been offset for clarity. The origin of each curve is shown by dashed lines.

this sample on the aisle of the quantum dot intersublevel absorption. The observation of the peaked resonance associated with the slow light mode for this periodicity is hindered by the noise of the measurement for this sample.

This work was partly supported by the French National Research Agency under the Contract No. ANR-PNANO QUOCA.

- <sup>1</sup>K. W. Berryman, S. A. Lyon, and M. Segev, *Appl. Phys. Lett.* **70**, 1861 (1997).
- <sup>2</sup>J. Phillips, K. Kamath, and P. Bhattacharya, *Appl. Phys. Lett.* **72**, 2020 (1998).
- <sup>3</sup>S. Sauvage, P. Boucaud, T. Brunhes, V. Immer, E. Finkman, and J. M. Gerard, *Appl. Phys. Lett.* **78**, 2327 (2001).
- <sup>4</sup>P. Boucaud and S. Sauvage, *C. R. Phys.* **4**, 1133 (2003).
- <sup>5</sup>P. Aivaliotis, L. R. Wilson, E. A. Zibik, J. W. Cockburn, M. J. Steer, and H. Y. Liu, *Appl. Phys. Lett.* **91**, 013503 (2007).
- <sup>6</sup>J. Jiang, K. Mi, S. Tsao, W. Zhang, H. Lim, T. O'Sullivan, T. Sills, M. Razeghi, G. J. Brown, and M. Z. Tidrow, *Appl. Phys. Lett.* **84**, 2232 (2004).
- <sup>7</sup>D. Z.-Y. Ting, S. V. Bandara, S. D. Gunapala, J. M. Mumolo, S. A. Keo, C. J. Hill, J. K. Liu, E. R. Blazewski, S. B. Rafol, and Y.-C. Chang, *Appl. Phys. Lett.* **94**, 111107 (2009).
- <sup>8</sup>S. Sauvage, P. Boucaud, T. Brunhes, A. Lemaitre, and J. M. Gerard, *Phys. Rev. B* **60**, 15589 (1999).
- <sup>9</sup>F. Bras, P. Boucaud, S. Sauvage, G. Fishman, and J. M. Gerard, *Appl. Phys. Lett.* **80**, 4620 (2002).
- <sup>10</sup>P. Boucaud, S. Sauvage, and J. Houel, *C. R. Phys.* **9**, 840 (2008).
- <sup>11</sup>E. Yablonovitch, *Phys. Rev. Lett.* **58**, 2059 (1987).
- <sup>12</sup>K. Sakoda, *Optical Properties of Photonic Crystals* (Springer, Berlin, 2005).
- <sup>13</sup>T. Baba, *Nat. Photonics* **2**, 465 (2008).
- <sup>14</sup>R. Colombelli, K. Srinivasan, M. Troccoli, O. Painter, C. F. Gmachl, D. M. Tennant, A. M. Sergent, D. L. Sivco, A. Y. Cho, and F. Capasso, *Science* **302**, 1374 (2003).
- <sup>15</sup>L. Sirigu, R. Terazzi, M. I. Amanti, M. Giovannini, J. Faist, L. A. Dunbar, and R. Houdré, *Opt. Express* **16**, 5206 (2008).
- <sup>16</sup>A. Benz, C. Deutsch, G. Fasching, K. Unterrainer, A. M. Andrews, P. Klang, W. Schrenk, and G. Strasser, *Opt. Express* **17**, 941 (2009).
- <sup>17</sup>S. Sauvage and P. Boucaud, *Appl. Phys. Lett.* **88**, 063106 (2006).
- <sup>18</sup>E. Homeyer, J. Houel, X. Checoury, G. Fishman, S. Sauvage, P. Boucaud, S. Guilet, R. Braive, A. Miard, A. Lemaitre, and I. Sagnes, *Phys. Rev. B* **78**, 165305 (2008).
- <sup>19</sup>T. Muller, W. Parz, K. Unterrainer, S. Sauvage, J. Houel, P. Boucaud, A. Miard, and A. Lemaitre, *Phys. Rev. B* **77**, 035314 (2008).